Extrusion foaming of poly(lactic acid) blown with CO_2 : Toward 100% green material

Reignier, Joël; Gendron, Richard; Champagne, Michel F.

Publisher's version / Version de l'éditeur:

Cellular polymers, 26, 2, pp. 83-115, 2007-01-01

Extrusion Foaming of Poly(Lactic acid) Blown with CO_2: Toward 100% Green Material

Joël Reignier, Richard Gendron and Michel F. Champagne
Industrial Materials Institute, National Research Council Canada
75, de Mortagne, Boucherville, QC, Canada, J4B 6Y4
Tel: 1-450-641-5183, Fax: 1-450-641-5105, E-mail: michel.champagne@cnrc-nrc.gc.ca

ABSTRACT

This paper presents a thorough investigation of the continuous extrusion foaming of amorphous poly(lactic acid) (PLA) using carbon dioxide (CO_2) as the blowing agent. Detailed results describing the plasticization induced by CO_2 dissolution as measured from two different methods, on-line rheometry and in-line ultrasonic technique, are given. Characteristics of the foams obtained from extrusion performed under various processing conditions are also reported. Extrusion of PLA foams in the 20-25 kg/m^3 density range was achieved. However, the associated processing window was very narrow: CO_2 content lower than ca. 7 wt% did not lead to significant foam expansion while foams blown at CO_2 contents larger than 8.3 wt% showed severe shrinkage upon ageing.

Key Words

Biodegradable polymers; poly(lactic acid); foam extrusion, open-cell, plasticization.

INTRODUCTION

In the last decade, there have been considerable efforts devoted to the development of polymers from renewable agricultural resources in order to gradually replace traditional polymers made from non-renewable fossil resources such as polystyrene or polyethylene. Among those, poly(lactic acid) (PLA), conventionally considered as a relatively expensive synthetic polymer dedicated exclusively to

biomedical applications, can now be produced at low cost, typically *ca.* 1.50 US$/pound. Biotechnology breakthrough enables corn-based feedstock transformation into high-quality PLA polymer [1]. Thus, PLA is being currently commercialized in large quantity for targeted implementation in fiber and packaging applications. An extensive review on the physical properties of PLA indicates that it is a good candidate for packaging applications [1]. PLA can be molded, blown, or extruded to yield products which were traditionally made from petroleum-based plastics. When composted, PLA can be degraded down to its basic natural component, lactic acid, readily assimilated by bio-organisms commonly found in nature, thus making the polymer biodegradable.

Until recently, foaming of PLA was restricted exclusively to biomedical applications. Indeed, both tissue engineering and guided tissue regeneration required the use of porous biodegradable polymeric materials. Pioneering study on the foaming of poly(D,L-lactic-co-glycolic acid) (PLGA) with CO_2 as blowing agent was done by Mooney *et al.* [2] using batch processing at ambient temperature. Interestingly, they demonstrated that the porosity (in other words the density) of the foam could be controlled by mixing crystalline and amorphous polymers. Following studies aimed at improving such technology through better control of cell population density and cell size [3] and/or by incorporating encapsulated proteins [4].

The issue of PLA foaming for non biomedical applications has been recently addressed by several researchers [5,6,7], through studies performed mostly using batch processes such as the autoclave method. Iannace's group carried out a number of interesting studies on the foaming of semi-crystalline biodegradable poly(ε-caprolactone) (PCL) and PLA with a 20:80 CO_2:N_2 mixture as physical blowing agent [6]. In addition, they proposed a strategy to increase the poor rheological properties and small processing window of the PLA foams by either adding nanoclays or through reactive processing (chain extenders and/or peroxides). In both cases, the foams exhibited reduced cell size and increased cell density (at foaming temperature of 110°C). Using a similar approach, Fujimoto *et al.* [5] reported the preparation and characterization of semi-crystalline PLA/layered silicate nanocomposite foams using only CO_2 as the blowing agent. They claimed that the more uniform cell morphology exhibited by the nanocomposite foam (foaming temperature of 140°C) compared to neat PLA foam may be explained by the presence of dispersed silicate particles acting as nucleating sites for cell formation. Surprisingly, the role of crystallization on the bubble nucleation was not addressed whereas a lot of studies have pointed out that CO_2 gas molecules can induced crystallization of the PLA matrix [8]. This issue may greatly

affect the interpretation of the previous data since it is difficult to separate the effect of nanoclays from those of crystals on bubble nucleation and growth.

In a completely different approach, numerous research efforts have been made to commercialize starch-based foams, in order to replace loose-fill packaging materials traditionally prepared from petrochemical products such as expanded polystyrene. Unfortunately, packaging materials made of pure starch show properties unacceptable for these applications: low moduli and strength and, even worse, solubility in water. To overcome this issue, several researchers have attempted in the last decade to improve the characteristics of starch-based foams by blending starch with oil-based polymers. Unfortunately, they generally relied on non-biodegradable polymers to provide the foam functionality. Therefore, there has been a growing interest in the development of completely biodegradable foams i.e. by mixing starch-based material with biodegradable polymers such as PCL, PLA and poly(hydroxy ester ether) (PHEE). Extruded foams made of starch blended with PLA (up to 40 wt.%) had significantly lower densities and larger radial expansion than control foams made from neat starch [9,10]. Compared to pure starch foams, the addition of PLA contributes to increase the elasticity of the cell walls thus preventing the cell structure to collapse [9] and improving the ultimate tensile strength and the percentage of elongation at break of the foam products [11]. Even if addition of PLA would significantly increase the cost of raw material – starch is ten times cheaper than PLA resins – the use of pure PLA foams may have a great potential in other packaging applications such as dinnerware, food containers and take-away products.

While batch processing enables valuable small-scale studies, scale-up towards industrial applications requires mass-production methods like the foam extrusion process. The specific characteristic of this process must then be taken into account. Therefore, the overall objective of this work was to investigate the continuous extrusion foaming of PLA with carbon dioxide (CO_2) as the single blowing agent, over a wide range of CO_2 concentrations. The rationale for combining PLA with an environmentally friendly blowing agent such as carbon dioxide is to generate a greener-type material since CO_2 would replace any conventional physical foaming agents (PFA), either organic or hydrofluorocarbon, that would otherwise directly enter the atmosphere.

EXPERIMENTAL PROCEDURE

Materials

The PLA resin, grade 8302D, was purchased from NatureWorks™. It is worth noting that the lactide monomer used to produce PLA has two enantiomers, L and D. Control of the ratio between L and D components is of critical importance since it has a large impact on the material properties. For instance, PLA derived from greater than 93% L-lactic acid can be semi-crystalline whereas PLA with L-lactic acid content ranging from 50 to 93% are totally amorphous. According to the supplier, the PLA grade 8302D is a completely amorphous copolymer made up of L- and D,L-lactide with a D- content of 9.85%. Some other physical characteristics of the PLA used in this study are reported in Table 1. Since amorphous PLA requires drying at temperature below its T_g, the PLA was dried for around 8h in a dryer set at 50°C prior to extrusion. Such drying stage is reported to be sufficient to decrease the moisture level below 250 ppm and thus to prevent hydrolysis of PLA in the molten state. In selected foam formulations, talc (Mistron Vapor-R from Luzenac Corporation) with a median particle size of 2 μm and a specific surface of 13.4 m^2/g was used as nucleating agent. The concentration of nucleating agent in the melt was set to 0.5 or 1 wt.%.

Foam Extrusion and In-line Characterization

The foam samples were prepared using a Leistritz 50 mm counter-rotating twin-screw extruder equipped with a 2 mm strand die having a L/D ratio of 0.5. The nominal flow rate was set to 15 kg/h. The in-line characterization was performed using an instrumented slit channel (pressure, temperature and ultrasonic probes) and an on-line rheometer (PCR, from Rheometric Scientific), both located between the twin-screw extruder and a gear pump (GP) as reported in Figure 1. This gear pump enables the control of the pressure inside the instrument slit channel. Both of these equipments have proven in the past to provide valuable information with respect to the whole thermoplastic foaming process, in particular on the degree of plasticization of the polymer matrix as function of the physical blowing agent concentration [12,13,14].

Density Measurement

The density of highly expanded specimens (typically <500 kg/m^3) was determined by water volume displacement of a known mass of foam. High density samples (typically >500 kg/m^3) were measured by weighting the foam extrudate in air and in water, using a balance with a resolution of 10^{-4} g. In both

cases, the PLA extrudates were cut using a razor blade at ambient temperature since the glass transition temperature of PLA is around 55°C.

Morphology Observation and Image Analysis

A scanning electron microscope (SEM), Hitachi SR-4700, operated at 1 kV voltage, was used to examine the morphology of the foams after fracturing the extrudate in liquid nitrogen. The cross-section was coated with platinum using a sputter coater (Emitech K575X) operating at 10 mA for about 15 s under argon atmosphere. The average cell size of the foam was measured by image analysis. The cell population density, as defined by the number of cells per unit volume of the original unfoamed polymer, was evaluated using the following equation:

$$\beta \cong \frac{6\times10^{+12}\left[\left(\rho_p/\rho_f\right)-1\right]}{\pi d^3} \tag{1}$$

where β is the cell population density (cells/cm^3), d the average diameter of the cells (μm), ρ_p and ρ_f the densities of the unfoamed and foamed polymers respectively (g/cm^3). The mean cell wall thickness (δ in μm) was estimated using the following equation:

$$\delta = d\left[\left(\frac{1}{\sqrt{1-\left(\rho_f/\rho_p\right)}}\right)-1\right] \tag{2}$$

Dimensional Stability

The radial dimension of the foam extrudates was measured using a laser scan (Keyence LS-3100 & LS-3060) coupled to a custom-built LabView™ application.

Open-cell Content

The open-cell content was measured using a gas pycnometer (model Accupyc 1330). For each sample, at least three measurements were done. The applied pressure (N_2 gas) was set to a value as low as 34.5 kPa (5 psi) to minimize collapse of the cellular structure.

Compression Mechanical Test

The compression tests were performed using a computer-controlled Instron mechanical tester on cylindrical samples having a diameter varying between 12 and 14 mm and an initial length of 28 mm.

The crosshead speed was set to 1 mm/min for all samples. The load-displacement curves were monitored during these tests in order to estimate both the compressive modulus and the compressive strength of the various foams investigated. Note that the compressive modulus of elasticity, E, was obtained from the slope of the initial linear portion of the compressive stress-strain curve. The compressive strength, σ_y, was obtained from the compressive stress at the yield point, i.e. to the first point on the compressive stress-strain curve at which an increase in strain occurs without an increase in stress.

RESULTS AND DISCUSSION

Plasticization

For an amorphous resin, the plasticization of the polymer matrix by the gas molecules is one of the critical steps in continuous extrusion foaming since it allows the process to be conducted at a temperature close to the glass transition temperature, T_g, of the neat polymer. This contributes to the stabilization of the cellular structure: as the foaming agent phase separates from the matrix to form the bubbles, the resin forming the walls and struts undergoes a rapid viscosity increase that prevents any cell collapse. Unfortunately, there was no data available in the literature for the actual PLA/CO_2 system. Different techniques have thus been used in the present work to estimate the T_g reduction induced by CO_2 sorption.

In the first approach, the magnitude of the plasticization has been assessed through in-line measurement of the ultrasonic velocity (V_{us}) of the PLA/CO_2 mixtures using the instrumented slit die. Figure 2 reports the influence of CO_2 concentration on the sound velocity of PLA/CO_2 mixtures during extrusion conducted at three different temperatures. It is worth noting that these data were collected at pressures ranging from 10.2 to 16.2 MPa, pressures considered sufficiently high to prevent phase separation and cell nucleation inside the ultrasonic slit die for the gas concentrations investigated. Since the pressure largely influences the ultrasonic velocity, the data reported in Figure 2 were corrected at a constant value of 14.5 MPa through the knowledge of the dependence of V_{us} with respect to pressure and temperature. Clearly, for each temperature, the velocity decreases in an almost linear fashion with the CO_2 content. The variation of ultrasonic velocity for polystyrene as a function of CO_2 and measured using the same apparatus is also reported on Figure 2 for comparison purposes (data excerpted from Ref (15)). With a slope of about -13m/s/wt.%, the plasticization of CO_2 seems less pronounced with PLA than with PS

(≅ -17m/s/wt.%). As reported earlier by Gendron *et al.* [16], the decrease of sound velocity is proportional to the lowering of the glass transition temperature of the polymer due to the plasticizing effect of the dissolved gas. Therefore, these data can be used to estimate the shift in glass transition temperature due to the presence of the blowing agent by comparing the temperature/CO_2 content equivalence at a given constant value of ultrasonic velocity. Neglecting the variation in density with temperature and/or blowing agent content, the concentration dependence of the PLA T_g under flow conditions (in-line) can be approximated as -8°C/wt.% CO_2.

In the second approach, stress sweep tests were realized using the on-line rheometer in order to measure the effect of blowing agent concentration on the rheological properties of the PLA/CO_2 mixtures. Typical results of viscosity measurements, expressed as shear stress as a function of apparent shear rates, are reported in Figure 3 for two temperatures and various concentrations of CO_2. Note that the pressures prevailing inside the rheometer were maintained above 5 MPa to prevent phase separation and foaming. Due to rheometer pressure limitations, investigations were focused on CO_2 concentrations below 6-7 wt%. The viscosities reported herein correspond to those of homogeneous single phase mixtures of PLA and CO_2. The plasticization translates into the viscosity decrease of the polymer/blowing agent mixture with addition of CO_2 at any given temperature. For instance, addition of 4.9wt.% CO_2 leads to more than 50% viscosity reduction compared to the neat PLA at the same temperature (160°C, comparison made at constant stress). Making the assumption that the viscosity reduction upon addition of the blowing agent is mainly dependent upon the depression in T_g, one can estimate the T_g dependence on CO_2 content through viscosity-temperature equivalences. Obviously, the curves labeled "160°C - 1,7%" and "140°C - 4.7%" display almost similar viscosities, which suggests that each percent of CO_2 decreases the T_g by approximately 6°C. In other words, dissolving 10wt.% of CO_2 enables operation at temperatures 60°C cooler. For comparison purpose, Gendron *et al.* [17] reported a level of plasticization of –8°C/wt.% CO_2 for PS.

The depression of the glass transition temperature caused by absorption of diluent molecules can also be estimated using a theoretical relation developed by Chow [18], which is mainly based on the respective molecular weight of the diluent and the polymer repeat unit:

$$\ln\frac{T_g}{T_{g0}} = \psi\left[(1-\theta)\ln(1-\theta)+\theta\ln\theta\right] \tag{3}$$

where $$\theta = \frac{\omega / M_d}{z(1-\omega)/M_p} \quad (4)$$

and $$\psi = \frac{zR}{M_p \Delta C_p} \quad (5)$$

Here, T_{g0} is the glass transition temperature for the pure polymer, while T_g is the value function of the weight fraction of diluent ω. M_d and M_p are respectively the molecular weight of the diluent and that of the polymer repeat unit. ΔC_p is the change in specific heat of the polymer at its glass transition temperature and R the gas constant. The parameters for the PLA/CO_2 system used in the calculations were M_d=44g/mol, M_p=72g/mol, ΔC_p=0.548J/g/K and T_{g0}=328.3K. The lattice coordinate number, z, was set equal to 2. Figure 4 shows the evolution of T_g of PLA as a function of CO_2 weight content, as estimated from the different methods, including ultrasonic velocity and rheological measurements. While the approximation using Chow's approach does not take into account the possible chemical interactions between the two components, the results deduced from extrusion experiments suggest clearly an affinity between PLA and CO_2 which yields to a significant plasticization enhancement. Nevertheless, despite the fairly large discrepancy at high CO_2 content between the various investigation techniques, a strong dependence of the T_g of PLA with the concentration of CO_2 should be kept in mind.

Solubility Measurements

Solubility of the gas into the polymer matrix is also a key parameter in foam processing. Although equilibrium solubility can be very accurately measured using sophisticated techniques such as a magnetic suspension electrobalance, these measurements remain tedious which may explain the small amount of results reported in the literature. On the other side, a fair and quick estimate can be provided from extrusion experiments by monitoring the pressure at the injection point in the barrel. Assuming the twin-screw extruder to be starve-fed at the injection point, the blanket of blowing agent in the extruder barrel should then be in equilibrium with the polymer melt at this injection point. In that case, the injection pressure (P_2 in Figure 1), as depicted in Figure 5 for the PLA/CO_2 system at three nominal melt temperatures of 90, 100 and 110°C (as set at the die exit), should correspond to the equilibrium solubility. Clearly, the injection pressure varies almost linearly with the concentration of CO_2 investigated. Note that our assumption is confirmed by extrapolation of the linear fit from our experimental results (solid line) at $P_{inj} \cong 0$ for a CO_2 content of 0 wt.%. In addition, the solubility of CO_2 in PLA seems not to be affected by the addition of talc (filled symbols in Fig. 5). For comparison

purpose, solubility data extrapolated from work done by Sato *et al.* [8] are reported herein for a temperature of 130°C (dashed line). Obviously, the temperature prevailing at the barrel section preceding the injection point should be around 140°C, which is normally higher than the reported nominal temperature set at the die exit.

Unexpected degassing inside the gear pump occurred while processing under very high concentrations of CO_2, i.e. near 10wt%, despite the fact that the suction pressure of the gear pump was set to a value compatible with the injection pressure. While an injection pressure of approximately 10 MPa is typically needed to dissolve 9.5 wt.% of CO_2, suction pressures as high as 20.7 MPa were required to prevent degassing inside the gear pump and extruder during such extrusion performed at high carbon dioxide content. These very high processing pressures consequently limited the maximum gas concentration investigated, since higher pressures at the gear pump entrance involves filling up the extruder to a larger extent and this modifies considerably the extrusion conditions. These limitations are essentially equipment-related and it is thermodynamically possible to dissolve more CO_2 in PLA using different conditions.

Foam Density and Morphology

Effect of Blowing Agent Content

To investigate the effect of blowing agent concentration on the density and cell morphology of the extruded foam, the CO_2 content was increased stepwise from 1.8 to 9.4 wt.% by *ca.* 1 wt.% increment. It is worth noting that all the in-line characterization equipments (ultrasonic instrumented die and on-line rheometer), acting as flow rectrictors, were removed to better control the pressure prevailing inside the extruder and to ease the increase of the suction pressure at the entrance of the gear pump to values as high as 20.7 MPa. As mentioned in the previous section, these extra precautions were taken to avoid premature foaming inside the gear pump at high CO_2 concentrations. Indeed, it has been shown recently that the degassing pressure – i.e. the pressure at which bubble nucleation and growth begins – may increase significantly under flow conditions well above the equilibrium solubility associated value because of the shear and tensile stresses induced during flow [19].

Figure 6(a) displays the foam density variation as a function of blowing agent concentration for a nominal processing temperature of 100°C. Average cell sizes calculated by image analysis as well as estimation of cell population density (according to Eq.1) have been plotted as a function of CO_2 content in Figure 6(b)-(c). SEM micrographs corresponding to the various foaming agent concentrations with or without talc are shown respectively in Figures 7 and 8.

Three distinct regions can be distinguished in Figure 6, with respect to various blowing agent concentrations (low, moderate and high):

Region I: At low blowing agent concentration, typically lower than 5 wt.% CO_2, it can be clearly seen that the CO_2 content has a limited impact on the density reduction of the neat PLA. The foam density remains high with values above 500 kg/m^3. The corresponding cell population densities are almost constant and rather small, with values typically less than 10^5 cell/cm^3 based on unfoamed material, which thus indicates a poor nucleation of the PLA/CO_2 system without nucleating agent. As shown in Figure 7(a), the cellular structure of the 1.9 wt.% CO_2 foam sample is very poor with macroscopic bubbles irregular in shape. Figure 7(b) illustrates that increasing the concentration of blowing agent to 4.3 wt.% induces more uniform spherical cells that remain still isolated.

Region II: Increasing the blowing agent concentration from approximately 5 to 7 wt.% CO_2 has a marked effect on the cellular morphology. The bulk density of the foam drops abruptly while the cell population shoots straight up by almost three orders of magnitude. The micrograph reported in Figure 7(c) indicates that cells now interact with each other and are no longer spherical in shape. This corresponds to a transition zone.

Region III: Eventually, above 7 wt.% CO_2, low density foams can be achieved (less than 30 kg/m^3) and foam density does not change significantly with CO_2 content while the cell population density slightly increases with CO_2 from 10^7 to 10^8 cell/cm^3. The corresponding foam morphologies depicted in Figures 7(d)-(f) reveal regular hexagonal bubbles with an average diameter in the 200-400 μm range, with the cell size decreasing with increasing CO_2 content. A few open cells are visible in all cases. It appears from the above results that a critical gas concentration of 7 wt.% is required for a favorable nucleation and expansion process leading to low density foams, in absence of any nucleating agent. This concentration threshold will be discussed later in the paper.

Effect of Talc on Cellular Structure

The effect of talc addition on cell density and cell morphology is considered next. Addition of 0.5 wt.% talc to foam formulations clearly leads to a much finer cell morphology in regions I and II, indicative that talc particles act as heterogeneous nucleation sites for bubble nucleation. The cell population density increases by a factor 100 while the average size drops from a few hundreds micrometers down to less than 60 μm. Foam morphologies presented in Figures 8(a)-(b) show a clear trend of decreasing cell sizes with respect to neat PLA at the same content of CO_2 (see Figures 7(a) and (c), respectively).

However, at higher carbon dioxide concentrations (region III), the effect of talc on the morphology of the cellular structure vanishes since there is no longer significant difference between the foam density, cell population density and average cell size for the samples processed with or without talc. This point will be discussed in more details in the next section.

Foaming PLA with CO_2 near Supercritical Conditions

The most striking fact displayed in Figure 6(a) is the critical foaming agent concentration below which foam expansion remains very low. Note that a similar observation have been reported for polycarbonate (PC) blown with CO_2 [20]. Above this critical value, i.e. *ca.* 7 wt.% CO_2, significant expansion occurs and foam density decreases abruptly down to approximately 20 kg/m^3. For instance, the foam density obtained at 100°C for a CO_2 concentration of 6.4 wt.% is slightly higher than 700 kg/m^3, which is only half the density of pure PLA, despite the high concentration of blowing agent used. Similar results, not reported here, have also been obtained at 90°C.

The processing window associated to "good foams" (honeycomb structure and density lower than 40 kg/m^3) is reported in Figure 5 by a shaded area. Interestingly, the processing window associated with low density foams and high nucleation rate (10^7-10^8 cell/cm^3) involves an injection pressure (for the associated required gas concentration) that corresponds relatively well to the critical pressure of CO_2 (7.38 MPa). Based on several abnormal features observed during extrusion foaming involving various polymer/PFA combinations, it has been recently proposed [21] that processing a physical blowing agent under conditions that are close to or slightly above its critical point (i.e. at a temperature greater than its critical temperature T_c and at pressure around its critical pressure P_c) could dramatically affect the cell nucleation due to the presence of local density inhomogeneities of the physical blowing agent. At this point, it is still not clear if this strange behavior could be a reminiscence of the supercritical state of the blowing agent prevailing during its injection or to the physical state of the PFA during the phase separation stage.

Recently reviewed by Tucker [22], the issue of solvent density inhomogeneities in supercritical fluids (SCF) are of primary importance in the development of new chemical processes based on control of solvation properties. Density variations of *ca.* 20% have been reported [23] in pure SCF. However, it has been demonstrated in dilute supercritical solutions – in that case, a very low concentration of polymer is introduced into the solvent - that additional inhomogeneities exist leading to local density that may be 2-3 times that of the bulk density [23]. In addition, the magnitude of these local inhomogeneities was found to be related to the intensity of solute-solvent interactions [23]. According to Urdahl *et al.* [24], this

particular behavior may be seen as a liquid-like condensation, i.e. a localized phase transition of the fluid molecules around the solute polymer because the attractive solute-solvent interaction would be greater than that between the solvent molecules. Such local inhomogeneities would likely act as powerful nuclei for initiating bubble nucleation.

In another approach, Cotugno *et al.* [25] reported on the formation of macroscopic fluid bubbles (visible through the window of a high pressure view cell) in molten PCL/CO_2 system upon increase of the CO_2 pressure inside the chamber. They proposed that this phase separation would be intimately linked to a pressure effect for the fluid in its supercritical state. Melnichenko *et al.* [26] addressed the effect of temperature and pressure on the phase behavior of poly(dimethylsiloxane) (PDMS) diluted in CO_2 using small angle neutron scattering (SANS). They reported the first experimental observation that an increase in pressure in supercritical polymer solutions can induce demixing. This polymer-solvent phase separation would correspond classically to the lower critical solution temperature observed for phase diagram of polymers in inorganic solvents. In a different approach, a few authors [27,28] reported swelling anomalies, explained by an onset of phase separation, in polymer thin films exposed to CO_2 near its critical point. Again, the high pressure associated with CO_2 supercritical state processing would favor the generation of small CO_2 clusters acting as bubble nuclei, thus leading to good foams in these conditions.

Another clue on the enhanced nucleation reported when the blowing agent is injected near its supercritical state is given by comparing the effect of talc on cell nucleation density before and near the critical region. Interestingly, while the effect of talc as nucleating agent is clearly visible for CO_2 concentrations lower than 5 wt.%, it seems to vanish at higher concentration of CO_2 (see Figure 6(b)). However, it does not necessarily mean that talc particles cannot play the role of nucleating agent since increase of the cell population density by an absolute value of *ca.* 10^7 cell/cm^3 – as observed at low CO_2 content – would be barely apparent on a log scale at a nucleation level greater than 10^8 cell/cm^3. The cell nucleation rate in homogeneously nucleated systems reaches its maximum value near the critical conditions.

Two different hypotheses can explain these results:

(i) By analogy with crystallization from the molten state where the nucleation efficiency of various nucleating agents can be ranked in percent between non-nucleated and "ideally nucleated" (i.e self-nucleation) [29], the best nucleating agent for cell nucleation will be a cluster or a stable nuclei of the blowing agent itself.

(ii) As shown in static conditions, phase separation in a binary polymer/PFA system does not necessarily occur at the binodal curve, which corresponds to the equilibrium solubility [30]. In other words, the system could enter in a metastable zone at lower pressure and stay some time in a supersaturated state before experiencing phase separation. However, at higher concentration of blowing agent, the metastable region, expressed in terms of ΔP, is reduced and even vanishes at the junction between the binodal and spinodal curves. Therefore, density fluctuations characteristic of spinodal decomposition would be higher for the same value of ΔP (supersaturation state) which would facilitate the formation of clusters. This mechanism would thus render talc inoperative for heterogeneous nucleation purposes.

From a processing point of view, foaming in the supercritical region was found to be generally problematic as it often renders the extrusion process unstable and leads to foams exhibiting an heterogeneous morphology made of large mm-sized cells dispersed in a microcellular morphology [21]. In our case, despite the fact that the foams resulting from an injection pressure (or equivalent concentration) approaching P_c varied widely in terms of physical characteristics from one run to the other (see Figure 6(a) and (c) at 6.4 wt.% of CO_2), the use of CO_2 at injection pressures higher than P_c (with T/T_c ratio close to 1.22) eliminates this product variation and greatly enhances the cell nucleation, thus leading to foam densities lower than 30 kg/m^3 with no blow holes. It then seems possible that polymer/PFA interactions are one of the key parameters to explain the above discrepancy.

Dimensional Stability of Low Density PLA Foams

Significant changes in shape and dimensions of the extruded foams were observed during the post-extrusion ageing process of the low density foam samples. The pictures shown in Figure 9 provide a stricking example of the surface irregularities of a foam sample after a 48h storage at ambient conditions. The sample was extruded at a nominal temperature of 100°C and blown with 9.3 wt.% of CO_2.

Even if the former purposes of this study did not include the investigation of the basic mass transport and volume relaxation process, the dimensional stability of PLA foams was monitored as a function of post-extrusion time in order to give an insight on the kinetics of this shrinkage phenomenon. Figure 10(a) reports the evolution of strand diameter for the foam samples obtained at a nominal temperature of 100°C and for two blowing agent concentrations, 7.3 and 8.6 wt.% CO_2, which were found to exhibit very different dimensional stability behaviors during ageing. Note that the time zero corresponds to the moment when the sample was placed into the measuring system, i.e. typically within

15 minutes following the extrusion. The variation of each strand diameter is normalized with its respective initial diameter (t=0). In such a way, negative values indicate shrinkage of the extruded foams and extent of diameter reduction can be compared easily from one sample to the other without further calculation.

As shown in Figure 10(a), the kinetics and diameter reduction are completely different for the two samples. The sample blown with 7.3 wt.% CO_2 shrink only during the first 10 minutes ($6x10^2$s) with less than 1% variation. On the other side, the diameter of the sample blown with 8.6 wt.% CO_2 decreases continuously over 8h ($3x10^4$s) by more than 20%. For each system examined, the extruded foams were also allowed to age for at least two months, and no significant further change in their dimensions was observed compared to the large shrinkage happening in one case during the first 8h-period. Therefore, the shrinkage process was found to be permanent *i.e.* non-recoverable.

Based on the above data, all the foam densities of the specimens were reevaluated after two weeks and reported in Figure 11(a) as filled symbols. This time period was considered sufficiently long to ensure that the non-reversible shrinkage process was completed. Note that open symbols correspond to the density measurements performed immediately after the complete solidification of the extruded foam, typically within 15 min after extrusion, and obviously are the same as those reported in Figure 6(a) for the concentration range of 7.0-9.4 wt.% CO_2. Several densities were found to be significantly higher after ageing, and this effect is more pronounced for the highest CO_2 content. Obviously, these results are in agreement with the variation in strand diameter evidenced in Figure 10. Several papers have already treated this shrinkage issue for low-density foams, especially in the case of low density polyethylene foams [(31)] and PCL blown with CO_2 [(32)]. Works conducted over the past decade have shown that the contraction of the cellular structure is caused by the buildup of a negative pressure inside the cell cavities. This is due to differences in permeation rates of the blowing agent present in the closed-cell foam and exiting the foam faster than air (80% N_2) is entering into the cells. Since the reduction of the pressure inside the cells does not rupture the cell walls, the cellular structure collapse or shrink. Obviously, this phenomenon is amplified in low modulus foams.

More interestingly, the systematic difference in the density increase during the ageing process for concentrations of CO_2 varying between 7 and 9.3 wt.% is quite surprising. Since the initial density of the tested specimens is similar (21-24 kg/m^3), the mechanical response of the cellular structure to the internal negative pressure would be expected to be almost the same.

In order to investigate the reasons for such a difference, a thorough investigation of the dimensional – mass changes interrelationship is needed. Figure 10(b) depicts the mass variation during ageing for each of the system reported in Figure 10(a). Similarly, the mass change is normalized by dividing the variation in the sample mass by the initial mass of the extruded foam (t=0). Even though the exchange of gases after foam production started immediately as the foams underwent cooling, these experimental data indicate that gas diffusion out of the foam may still happen for a long period. However, the time required for the completion of gas mass transfer was found to strongly depend on the CO_2 content. More precisely, the sample with the highest concentration of CO_2 presents a mass reduction of more than 2.5 wt.% after over 5h (1.8×10^4s) of ageing whereas the decrease in the mass of the sample with the lowest content of CO_2 is approximately 1.4 wt.% after only 15 min (900s). Even if extrapolation is uncertain, the relative amount of gas lost during the transfer from the extruder to the balance should be higher for the lowest CO_2 content. The kinetics (initial slope of the curve) is clearly faster for lower CO_2 content foams when compared to samples made with larger CO_2 concentrations. Therefore, the plateau value corresponding to the lower CO_2 content should be shifted downward with respect to the curve corresponding to the higher CO_2 content and thus, it is not possible to determine which samples show the greater mass loss during ageing. Moreover, the above results cannot explain the dependence of the dimensional stability with CO_2 content. The only information available is that the time required to reach a constant and stable mass was found to be strongly dependent on the CO_2 concentration: the lower the CO_2 content is, the shorter the time to reach equilibrium will be.

Open-cell Content

For closed-cell structures, gas transport is initiated between the inner surface of the foam and the ambient air, and then propagates within the material cell by cell through two main modes of transport: (i) Permeation of the gas dissolved in the solid matrix through the cell walls and (ii) gas phase diffusion across the space inside the cells. However, the presence of open-cells interferes with the transport mode described above since the gas molecules are free to move (convection) through holes in cell walls, bypassing the diffusion step through the polymer network. Therefore, open-cells should obviously reduce the pressure gradients between the cells and accelerate the mass transport kinetic of the various gases in and out of the foam. Eventually, the dimensional stability of the foam should be affected by the content of opened cells. The open-cell content (OCC) was therefore measured immediately after the foams have been produced (typically within 30 min) and is reported in Figure 11(c) as a function of CO_2 content for the foams blown at a nominal temperature of 100°C. Figure 11(d) shows several holes in cell

walls for the PLA foam obtained with 7.3 wt.% CO_2 at 100°C (same sample as shown in Figure 7(d)). Clearly, the content of blowing agent significantly impacts the open-cell content. Increasing the CO_2 content from around 7.3 to 9.3 wt% reduces the open-cell content by a factor of 4. It is worth noting that it was not possible to characterize PLA foams having a CO_2 content higher than 9.1 wt.% since the dimensional change of these foam samples was too fast to allow a fair estimate of their OCC. In these latter cases, massive foam densification was observed even during the measurements in the gas pycnometer.

Obviously, Figure 11(b) evidences a slight but significant reduction in cell wall thickness with an increase of the CO_2 content. Adding more and more blowing agent increases the nucleation rate despite a reduction of the pressure drop rate (higher plasticization then lower melt pressure at the die). Note that the foam expansion ratio is almost the same within the concentration range reported in Figure 11. Surprisingly, comparing Figures 11(b) and 11(c) unambiguously shows that open-cell content decreases with a reduction in wall thickness. The opposite behavior would have been expected since cell opening is more likely to happen with thinner cell walls. This unexpected behaviour is probably reflecting the impact of CO_2-induced plasticization upon PLA melt extensional properties. Adding more and more CO_2 seems to increase PLA film resistance to rupture during the thin film stretching phase inherent to any low density foaming process.

It is also worth noting that the presence of talc does not have any significant impact on the open-cell content. Even if it is generally admit that adding talc increases the cell nucleation density through heterogeneous nucleation which in turn decreases the cell wall thickness (for a constant expansion ratio) and should then favor cell opening, this is not the case in our study since the cell population density is not significantly affected by the presence of talc (see Figure 6(b)) in this CO_2 concentration range.

More interesting, combining Figure 11(a) to 11(c) clearly evidences a relationship between densification (during ageing) and open-cell content. At low OCC (typically, between 20-30%), the density can increase by more than 100%, whereas the densification at higher OCC (above 40%) is limited to less than 10%. In other words, increasing the open-cell content seems to improve the dimensional stability of the foam but this relation does not necessary mean that the densification is solely controlled by the OCC. High OCC observed in the low concentration range may at least explain the faster permeation and thus the rapid dimensional stabilization of the foam produced.

Residual Plasticization

One possibility to explain the difference in the densification of the foams during ageing would be to consider the residual plasticization of the cell walls by dissolved CO_2 "left behind" after foaming. Indeed, the CO_2 molecules are not only distributed as a gaseous phase in the closed cells but they are also dissolved into the polymer matrix present as cell wall and struts. Since the foam density is almost the same - the number of gas molecules used to effectively blow the polymer matrix should also be the same - one would expect the residual CO_2 dissolved in walls and struts to increase with the initial CO_2 content. Basically, increasing the level of plasticization of the PLA phase would decrease the glass transition temperature of amorphous PLA phase close to or even below the ambient temperature and the foam properties would then be significantly modified. The degassing kinetics would be accelerated since permeability of small molecules through a rubbery membrane is usually much faster than for a amorphous glassy material. Even worse, residual gases dissolved in the matrix would significantly decrease the mechanical properties of the foam sample.

Making the assumption that the extruded foams stop expanding when the cell gas pressure drops to about the pressure of environmental air and that the gas losses are negligible, the amount of CO_2 molecules χ_{cell} required to maintain a given pressure inside the cell wall can be estimated using a PVT model by the following expression:

$$\chi_{cell} = \frac{P_{\text{int}} W \left(1 - \frac{\rho_f}{\rho_p}\right)}{\rho_f RT} \tag{6}$$

where P_{int}=1.013x10^5 Pa is the pressure of CO_2 inside the cell at t=0, W=44.010 g/mol is the molar mass of CO_2, R=8.3145 J/mol/K is the universal gas constant, ρ_p=1.24g/cm^3 and ρ_f the density of solid and foam PLA respectively. The amount of CO_2 remaining in the cell wall χ_{wall} (wt.% with respect to the mass of PLA) can be estimated by

$$\chi_{wall} = \chi_{init} - \chi_{cell} \tag{7}$$

where χ_{init} is the initial weight fraction of CO_2 in the PLA/CO_2 mixture. Table 2 gives the estimated values of χ_{cell} and χ_{wall} as a function of CO_2 for a foaming temperature of 100°C. Clearly, the results listed in Table 2 seem to indicate that the content of CO_2 in the cell wall should increase with the initial

concentration of CO_2 in the PLA/CO_2 mixture. Care should be paid however to the absolute value of the residual CO_2 in the cell wall. In fact, the CO_2 pressure in the cell cavity can be less than ambient pressure as the foam continues to cool. Pressures in the range of 0.3-0.6 atmosphere have been reported in the literature. Furthermore, a few works on the modeling of thermal conductivity during ageing have demonstrated that the amount of blowing agent dissolved in the polymer phase can be very high compared to predicted value based on a PVT model. For instance, abnormally high concentrations of $CFCl_3$ (FC-11) in polyurethane (PU) foams, 10-75 times larger than the expected equilibrium solubility (with respect to the pressure of gas inside cavity), have been reported in the past [33]. More recently, Mei [34] used ^{19}F MAS NMR spectroscopy to quantitatively demonstrate that *ca.* 13 wt.% HCFC-142b and more than 23 wt.% CFC-12 of the initial blowing agent added during the foam production stay dissolved in the PS matrix. These values are well above the equilibrium solubility of HCFC-142b and CFC-12 in PS at ambient pressure. In the case of PU foams, it was demonstrated that about 27 wt.% of the HCFC-142b (based on the total amount of gas in the foam) remains dissolved in the solid polymer network of the fresh foam (before ageing), and this value can even increase up to 33-37 wt.% for samples stored during 7 years. More importantly, the study highlighted that in both cases the dissolved blowing agents (within cell walls and struts) are strongly held in the polymer matrix since significant loss of dissolved gas can only be found after ageing under extreme conditions, i.e. high temperature and/or small size sample. No explanation was given on the origin of this strange behaviour. The affinity between the blowing agents and the polymer may obviously play a significant role as well as a low diffusion coefficient of the blowing agent in the polymer matrix. In our case, the CO_2 molecules are rather small compared to HCFC or CFC molecules, and thus CO_2 molecules should diffuse out of the foam much more rapidly than HCFCs or CFCs. Nevertheless abnormally high concentrations of CO_2 dissolved in the polymer matrix may still be expected.

On the other side, it has been shown using Fourier transform infrared spectroscopy (FT-IR) that the electron pair on the carbonyl oxygen of poly(methyl methacrylate) (PMMA) exhibits specific interactions, most probably of Lewis acid-base nature, with the carbon atom of CO_2 molecules[35]. Even if these specific interactions seem to be relatively weak, they take part in the relative high solubility of CO_2 in PMMA, which is also observed with other polymers containing carbonyl groups such as PLA and polycarbonate (PC). Indeed, it is important to remind that gas sorption is not a purely physical phenomenon (free volume) but it mainly depends on specific interactions between gas/fluid and the polymer. More interestingly, Kazarian *et al.* [35] explained that these interactions can be responsible for the "partitioning" of the CO_2 molecules. At low saturation pressures, the CO_2 dissolved within the

polymer film interacts weakly with the available carbonyl groups of PMMA whereas non-specifically interacting CO_2 molecules dominates the spectrum at higher CO_2 pressures. In another study, Shieh *et al.* [36] clearly demonstrated that it is more difficult to desorb CO_2 from PMMA and PC than from PS because of the greater interaction of the carbon of CO_2 with the carbonyl group present in PMMA compared to the phenyl group of PS. This differential interaction explains the higher solubility of CO_2 in PMMA than in PS. Although CO_2 was assumed to be absent within aged-samples of PMMA based on weight data measurements, these authors surprisingly found a shift of the relaxation peak to lower temperatures using dynamic mechanical analyzer (DMA). Carbon dioxide molecules were still dissolved in PMMA film 6 months after CO_2 treatment. This plasticization effect was not found in the case of PS film, thus indicating that the presence of specific interactions between the fluid molecules and the polymer can lead to entrapment of these molecules within the polymer matrix and thus render the sample difficult to outgas.

Based upon the above discussion on specific interactions, it is obvious to wonder if residual plasticization could be found in PLA/CO_2 and explain the poor dimensional stability of some foamed specimens. To get more insight on the possible effect of residual CO_2 on the dimensional stability of the extruded foams samples through matrix plasticization, the mechanical properties of the PLA foams were investigated in compression testing at low strain rates ($\approx 6\times10^{-4}$ s^{-1}). Samples were tested immediately after they have been produced. Gibson and Ashby [37] have provided an extensive textbook on the structure-property relationship of various cellular solids. One of their major results is that foam mechanical properties are related to density through power-law relationships. The specific foams investigated here show very similar density with value ranging from 20.8 to 24.2 kg/m^3. Given such minute difference in density, one would not expect a large impact on the mechanical properties of these foams. However, as reported in Table 3 and Figure 12, there is a two-fold decrease in modulus while the density is only decreasing from 24.2 to 20.8 kg/m^3. Recently, Bureau and Gendron [38] refined the semi-empirical Gibson and Ashby's equations to take into account of foam cell size (d). They demonstrated that compressive properties (E and σ_y) scaled well with a so-called "microstructure-density parameter", ρ/d, using modified power-law relationships. It is then possible to improve foam mechanical properties by reducing the cell diameter while keeping the density constant. In the PLA foams investigated here, cell sizes decreases from 120 μm to 80 μm as the CO_2 content was increased from 7.3 to 9.4 wt.%. According to Bureau's model, the compressive properties should slightly increase upon such cell size reduction. However, the opposite behavior is observed here. On the other hand, decreasing the open cell

content should also lead to a slight but significant mechanical properties improvement [37]. But in our work, specimens exhibiting the lowest open cell content showed the lowest mechanical performance. There is thus no acceptable correlation between the foam modulus or strength and the density, cell size or open content for the samples investigated. Interestingly, plotting E and σ as a function of the CO_2 content leads to nice correlations. Both the modulus and strength decreases with the concentration of carbon dioxide used (see Table 2 and Figure 12). Specimens made at higher CO_2 content are believed to be softer due to a higher level of plasticization induced by the residual CO_2. Eventually, a higher plasticization of the cell wall would allow a larger contraction of the cells to release the stress (elastic recoverable deformation) stored in the polymer matrix, thus increasing the density of the foam during ageing.

CONCLUSIONS

From our experimental investigation of the extrusion foaming of PLA with CO_2, it can be concluded that:

(i) CO_2 plasticizes very efficiently PLA; glass transition temperature depressions were estimated between -6 and -8°C/wt% CO_2.

(ii) Very low density PLA foams, in the order of 20-25 kg/m^3, have been achieved using a CO_2 concentration in the 7-9 wt% PFA range. Surprisingly, foams having an intermediate density could not be obtained by reducing slightly the blowing agent concentration. Interestingly, the injection pressure associated with this critical concentration threshold ($CO_2 \cong 7$wt%) corresponds to the critical pressure of carbon dioxide. As a consequence, this system requires high processing pressures in order to prevent premature foaming, despite the reported high solubility of CO_2 into PLA.

(iii) Increasing the concentration of blowing agent beyond this critical point has no effect on the bulk density of the produced foam. However, high CO_2 content severely deteriorates the dimensional stability of the foam over time in the post extrusion ageing process. Our results show a clear relationship between open-cell content and foam dimensional stability. Plasticization of the PLA matrix by residual CO_2 molecules entrapped in the polymer network significantly soften the foam and contribute to the massive shrinkage of the cellular structure observed in this work.

ACKNOWLEDGEMENTS

The authors are grateful to Karine Théberge, Manon Plourde and François Vachon for their technical support. Joël Reignier is also particularly grateful to Jacques Tatibouët for fruitful discussions.

REFERENCES

1. R. Auras, R., Harte, B. and Selke, S. *Macromol. Biosci.*, 4, 835-864 (2004).
2. Mooney, D.J., Baldwin, D.F., Suh, N.P., Vacanti, J.P. and Langer, R. *Biomaterials*, 17, 1417-1422 (1996).
3. Sparacio, A. and Beckman, E.J. Generation of Microcellular Biodegradable Polymers Using Supercritical Carbon Dioxide. Chapter 11, *ACS Polymer Preprints,* 38 (1998).
4. Hile, D.D., Amirpour, M.L., Akgerman, A. and Pishko, M.V. *J Control. Released*, 66, 177-185 (2000).
5. Fujimoto, Y., Sinha Ray, S., Okamoto, M., Ogami, A., Yamada, K and Ueda, K. *Macromol. Rapid. Commun.*, 24, 457-461 (2003).
6. Iannace, S., Di, Y., Di Maio, E. and Marrazzo, C. *The 7th International Conference on Blowing Agents and Foaming Processes*, Stuttgart (2005).
7. Hu, X., Nawaby, A.V., Naguib, H.E. , Day, M. , Ueda, K. and Lia, X. *ANTEC 2005 Annual Technical Conference,* Boston, 2670 (2005).
8. Sato, Y., Yamane, M.,Sorakubo, A., Takishima, S., Masuoka, H., Yamamoto, H. and Takasugi, M. *The 21st Japan Symposium on Thermophysical Properties*, Nagoya, 196-198 (2000).
9. Fang, Q. and Hanna, M.H. *Cereal Chem.*, 77, 779-783 (2000).
10. Willett, J.L. and Shogren, R.L. *Polymer*, 43, 5935-5947 (2002).
11. Prechawoong, D., Peesan, M., Supaphol, P. and Rujiravanit, R. *Carbohydr. Polym.*, 59, 329-337 (2005)
12. Sahnoune, A., Tatibouët, J., Gendron, R., Hamel, A. and Piché, L. *J Cell Plast*, 37, 429-454 (2001).
13. Gendron, R. and Daigneault, L.E. Rheological Behavior of Mixtures of Polystyrene with HCFC 142b and HFC 134a. *J. Cell. Plast.*, 35, 221-246 (1999).
14. Tatibouët, J. Chapter 5 : Investigating Foam Processing in Thermoplastic Foam Processing – Principles and Applications. Edited by R. Gendron, CRC Press, 195-233 (2005).
15. Vachon, C. and Gendron, R. *Cell. Polym.*, 22, 75-88 (2003).

16. Gendron, R., Huneault, M.A., Tatibouët, J. and Vachon, C. *Cell. Polym.*, 21, 315-341 (2002).

17. Gendron, R., Champagne, M.F., Delaviz, Y. and Polaski, M.E. *ANTEC 2005 Annual Technical Conference,* Boston, 2650-2652 (2005).

18. Chow, T.S. *Macromolecules*, 13, 362-364 (1980).

19. Tatibouët, J. and Gendron, R. *J. Cell. Plast.*, 40, 27-44 (2004).

20. Lee, J.W.S., Wang, K. and Park, C.B. *Ind. Eng. Chem. Res.*, 44, 92-99 (2005).

21. Gendron, R., Reignier, J. and Champagne, M.F. *J. Cell. Plast. Paper submitted* (2006).

22. Tucker, S.C. *Chem. Rev.* 99, 391-418 (1999).

23. Song, W., Biswas, R. and Maroncelli, M. *J. Phys. Chem. A* , 104, 6924-6939 (2000).

24. Urdahl, R.S., Rector, K.D., Myers, D.J., Davis, P.H. and Fayer, M.D. *J. Chem. Phys.*, 105, 8973-8976 (1996).

25. Cotugno, S., Di Maio, E., Mensitieri, G., Iannace, S., Roberts, G.W., Carbonell, R.G. and Hopfenberg, H.B. *Ind. Eng. Chem. Res.* , 44,1795-1803 (2005).

26. Melnichenko, Y.B., Kiran, E., Wignall, G.D., Heath, K.D., Salaniwal, S., Cochran, H.D. and Stamm, M. *Macromolecules*, 32, 5344-5347 (1999).

27. Sirard, S.M., Ziegler, K.J., Sanchez, I.C., Green, P.F. and Johnston, K.P. *Macromolecules* , 35, 1928-1935 (2002).

28. Koga, T., Akashige, E., Reinstein, A., Bronner, M., Seo, Y.S., Shin, K., Rafailovich, M.H., Sokolov, J.C., Chu, B. and Satija, S.K. *Physica B*, 357, 73-79 (2005).

29. Fillon, B., Lotz, B., Thieery, A. and Wittmann, J.C. *J. Polym. Sci:,B, Polym. Phys.*, 31, 1395-1405 (1993).

30. Reignier, J., Tatibouët, J. and Gendron, R. *Polymer*, 47, 5012-5024 (2006).

31. Yang, T.C., Lee, K.L. and Lee, S.T. *J. Cell. Plast.*, 38, 113-128 (2002).

32. Di Maio, E., Mensitieri, G., Iannace, S., Nicolais, L., Li, W. and Flumerfelt, R.W., *Polym. Eng. Sci.*, 45, 432-441 (2005).

33. Brandreth, D.A. and Ingersoll, H.G. *J. Cell. Plast.*, 16, 235-238 (1980).

34. Mei Z. NMR Imaging and Spectroscopic investigations of Blowing Gases in Polymer Insulating Foams. Ph.D Thesis – University of British Columbia (1996).

35. Kazarian, S.G., Vincent, M.F., Bright, F.V., Liotta, C.L. and Eckert, C.A. *J. Am. Chem. Soc.*, 118, 1729-1736 (1996).

36. Shieh, Y.-T., Liu, K.-H. *J. Supercrit. Fluids*, 25, 261-268 (2003).

37. Gibson, L.J. and Ashby, M.F. Cellulars Solids Structure and Properties, 2nd ed., pp.510, Cambridge University Press, New-York (1997).

38. Bureau, M and Gendron, R. *J. Cell. Plast.* 39, 353-367 (2003).

Table 1: Selected properties of amorphous PLA8302D (according to NatureWorks data sheets).

D- content	**Density** at 23°C	T_g (°C)	**Tensile Strength**[a] (MPa)	**Tensile Modulus**[a] (GPa)
9.85%	1.24	55	60	3.5

[a] Measurements were made in our laboratory according to ASTM D690 (tensile mode)

Table 2: Estimation of residual CO_2 concentration in the cells (χ_{cell}) and dissolved in PLA matrix (χ_{wall}) after foaming. Calculations were made using Eqs.(6)-(7). Note that χ_{init} corresponds to the concentration of blowing agent injected in the polymer

χ_{init} (wt.%)	ρ_f (kg/m^3)	χ_{cell} (wt.%)	χ_{wall} (wt.%)
7.3	24.2	5.8	1.5
8.6	21.5	6.6	2.0
9.3	20.8	6.8	2.5

Calculations made at T=100°C

Table 3: Mechanical properties and physical characteristics of low density PLA foams blown from CO_2.

% CO_2 (wt.%)	ρ (kg/m^3)	d (μm)	Compression Modulus (MPa)	Compression Strength (MPa)
7.3	24.2	125	4.1	0.081
8.6	21.5	100	2.8	0.074
9.3	20.8	70	2.1	0.070

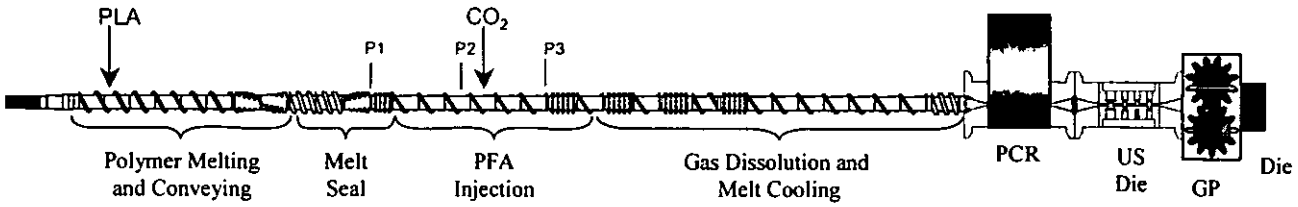

Figure 1: Schematic illustration of the setup, showing details of the screw configuration. Note that all the in-line and on-line characterization equipments (ultrasonic instrumented die and PCR) were removed to better control the pressure gradient inside the extruder during specimen preparation.

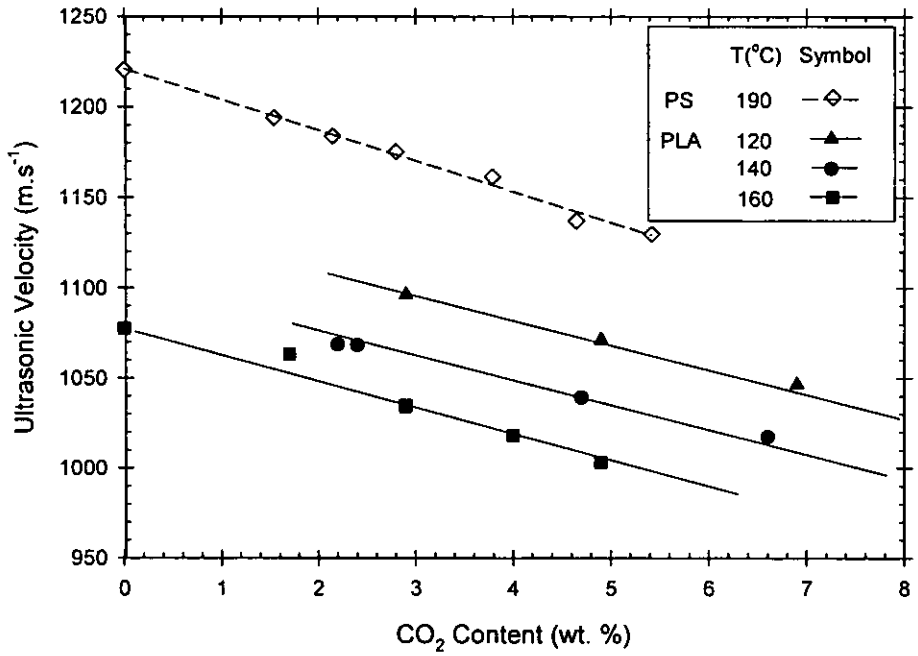

Figure 2: Ultrasonic velocity (homogenous single phase) as a function of CO_2 content dissolved in PLA for different nominal temperatures. The ultrasonic velocity values were corrected for pressure effects using a reference pressure of 14.5 MPa. The reported data for PS/CO_2 mixtures were taken from Ref (15).

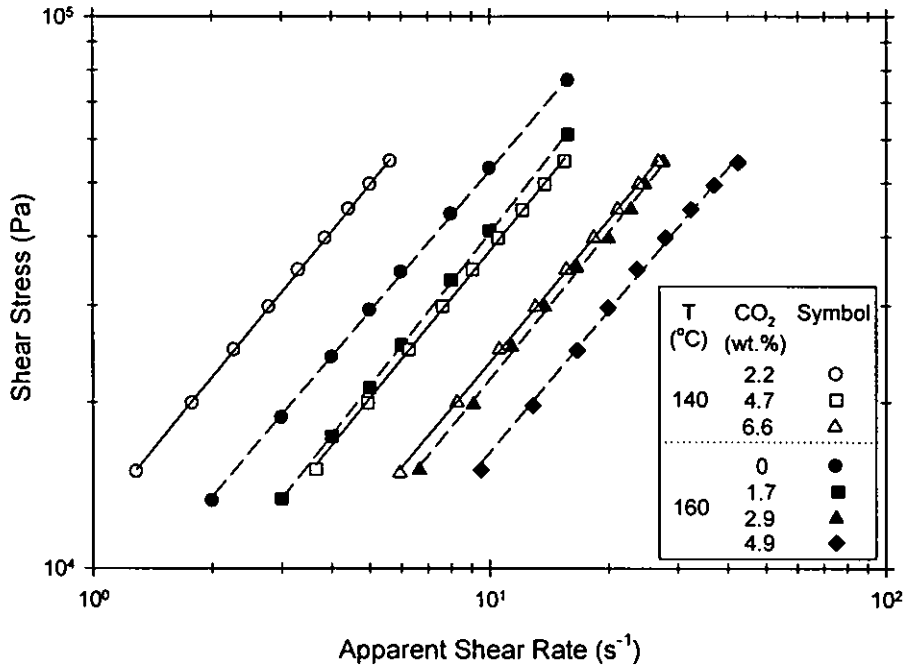

Figure 3: Apparent viscosity measurements of PLA/CO_2 mixtures at nominal temperatures of 140°C (open symbols) and 160°C (filled symbols) for various blowing agent contents.

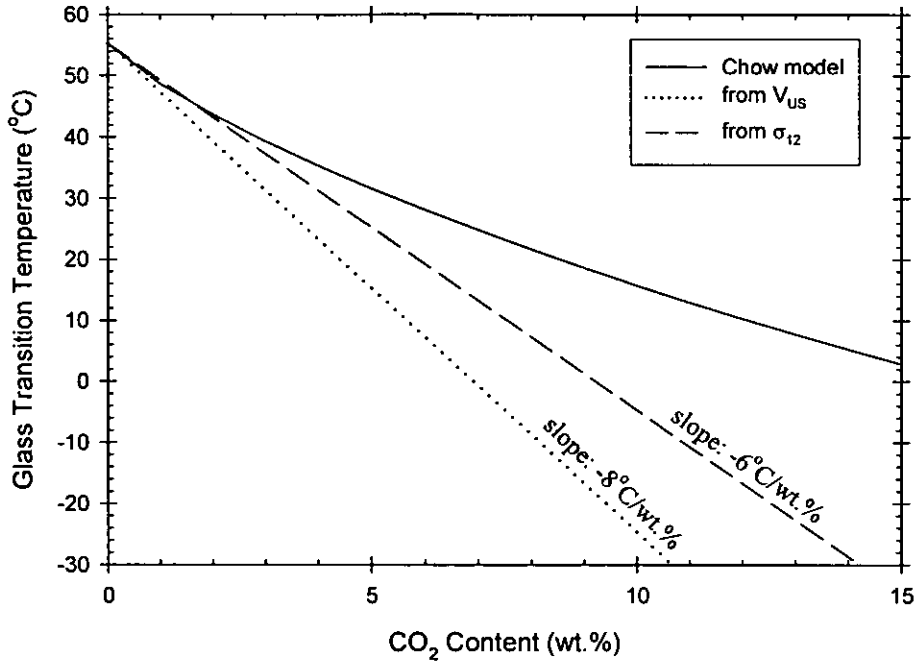

Figure 4: Variation of the glass transition temperature of PLA as a function of CO_2 content. The solid line corresponds to estimates using the Chow model with z=2. The dashed and dotted lines correspond to the depression dependence obtained from rheological and ultrasonic measurements, respectively.

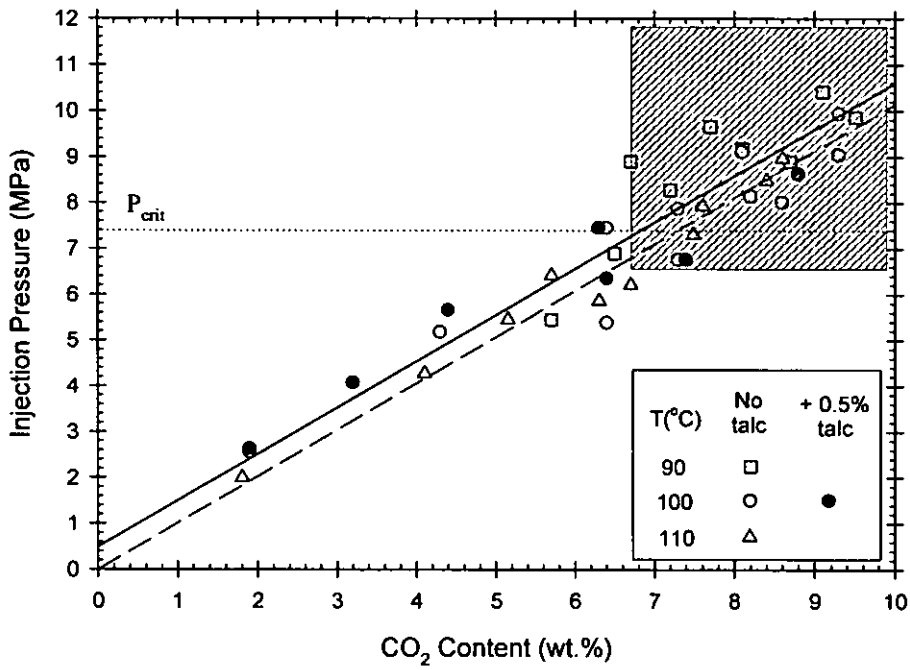

Figure 5: Influence of CO_2 content on the injection pressures (P_2 in Figure 1) as measured directly on the extruder. The solid line corresponds to linear fit of our data whereas the dashed line corresponds to equilibrium solubility data extrapolated at T=130°C from published data [8]. The shaded area corresponds to the "good low-density foam" processing window. The dotted line indicates the pressure level corresponding to the supercritical pressure of CO_2 (P_{crit}=7.386 MPa).

(a)

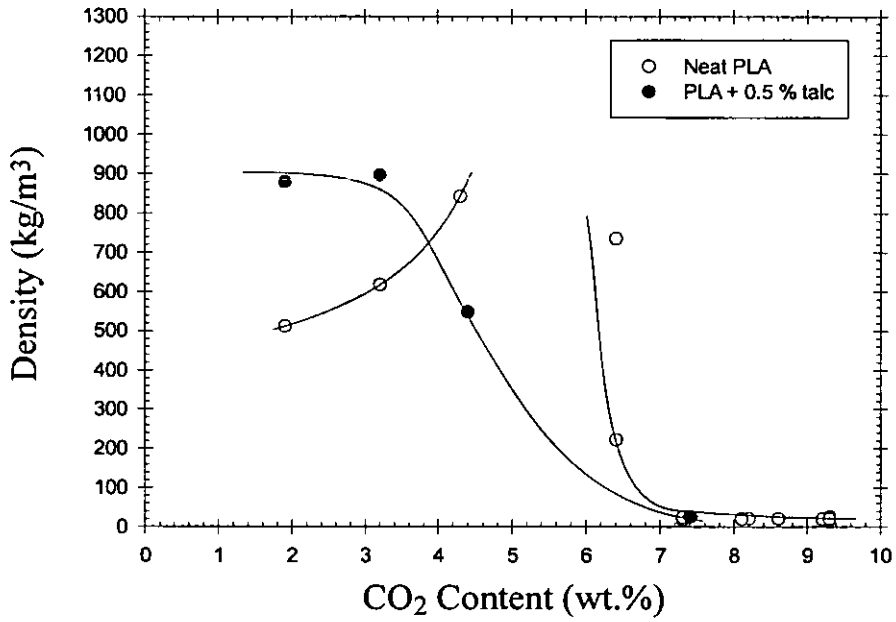
Neat PLA
PLA + 0.5 % talc
Density (kg/m3)
CO2 Content (wt.%)

(b)

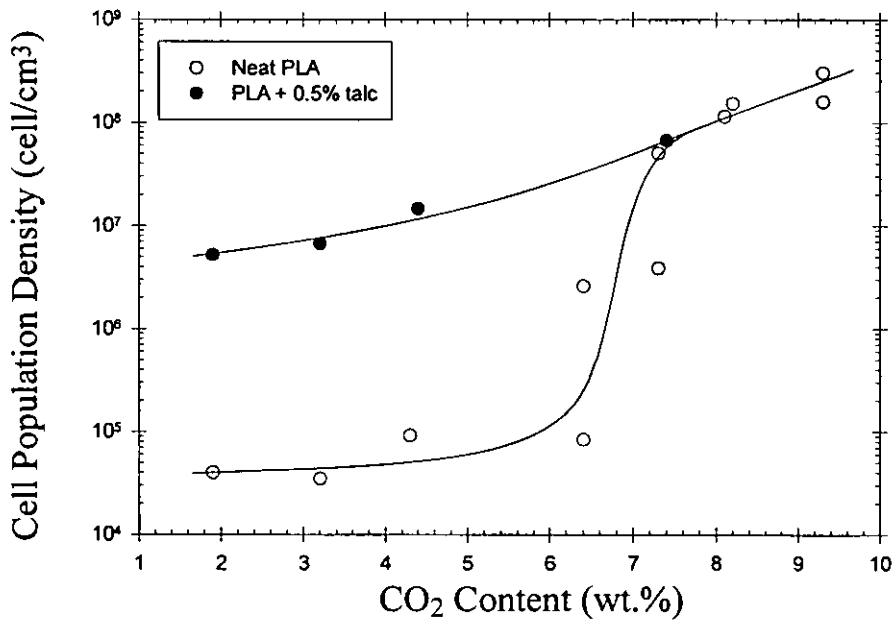
Neat PLA
PLA + 0.5% talc
Cell Population Density (cell/cm3)
CO2 Content (wt.%)

(c)

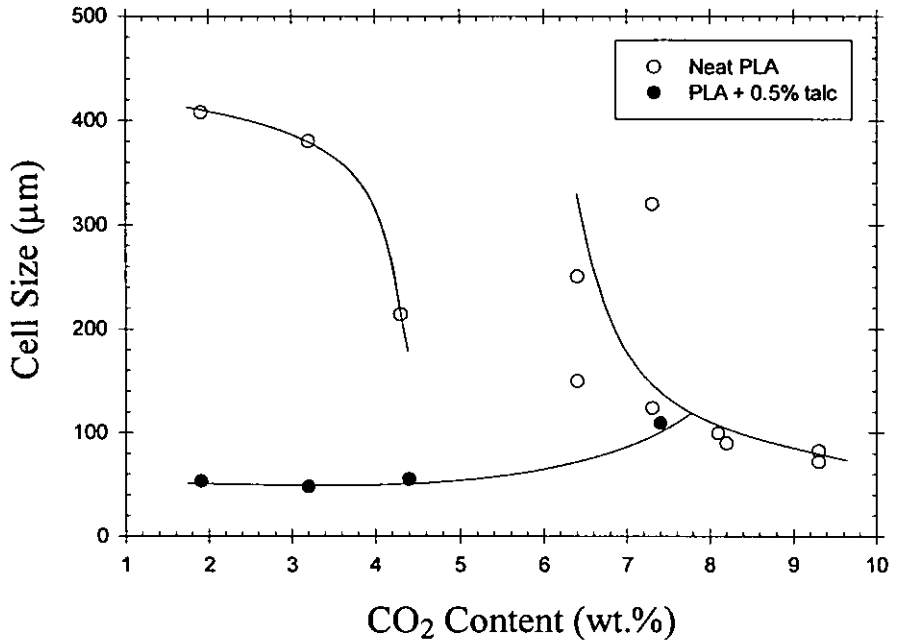

Figure 6: Effect of blowing agent concentration on (a) the bulk foam density; (b) the cell population density and (c) the cell size of neat PLA (open symbol) and PLA+0.5 wt.% talc (filled symbol) foams with CO_2 as blowing agent. Specimens were processed at a foaming temperature of 100°C. The lines are only guides for the eyes. Note that the density values reported here correspond to measurements made prior to samples ageing, typically within *ca.* 15 min after production.

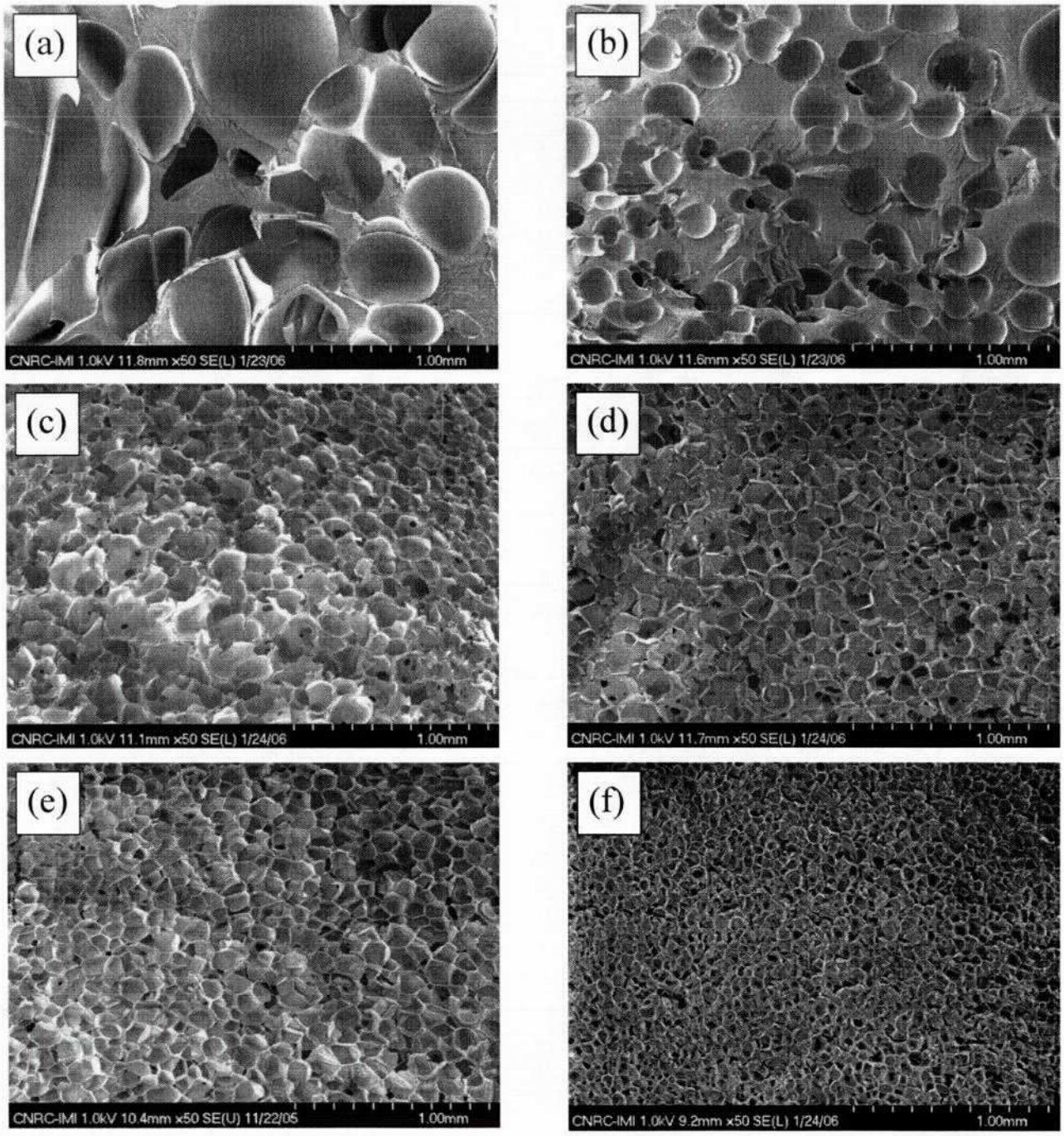

Figure 7: SEM photomicrographs of PLA foams obtained at a nominal temperature of 100°C using various concentrations of CO_2: (a) 1.9 wt.% - ρ=510 kg/m^3; (b) 4.3 wt.% - ρ=840 kg/m^3; (c) 6.4 wt.% - ρ=220 kg/m^3; (d) 7.3 wt.% - ρ=24 kg/m^3; (e) 8.2 wt.% - ρ=21 kg/m^3 and (f) 9.3 wt.% - ρ=21 kg/m^3.

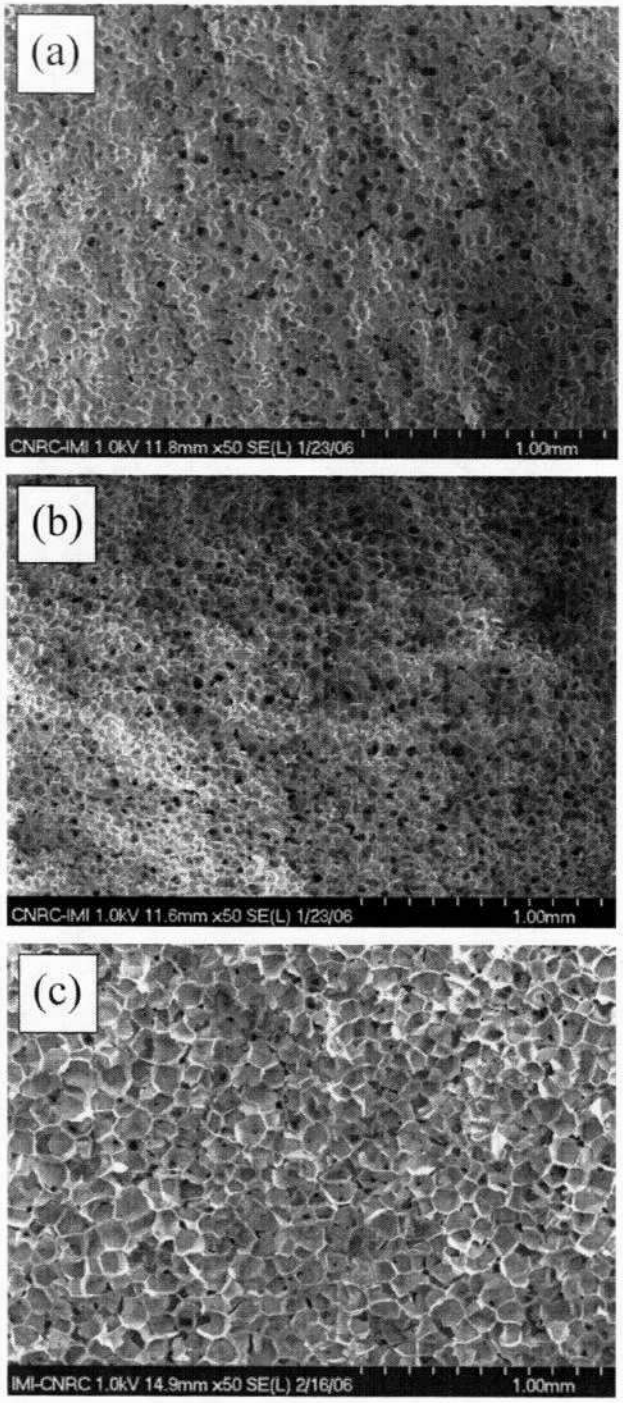

Figure 8: SEM photomicrographs of PLA+0.5 wt.% talc foams obtained at a nominal temperature of 100°C using various concentrations of CO_2: (a) 1.9 wt.% - ρ=880 kg/m^3 ; (b) 4.3 wt.% - ρ=550 kg/m^3 and (c) 7.3 wt.% - ρ=33 kg/m^3

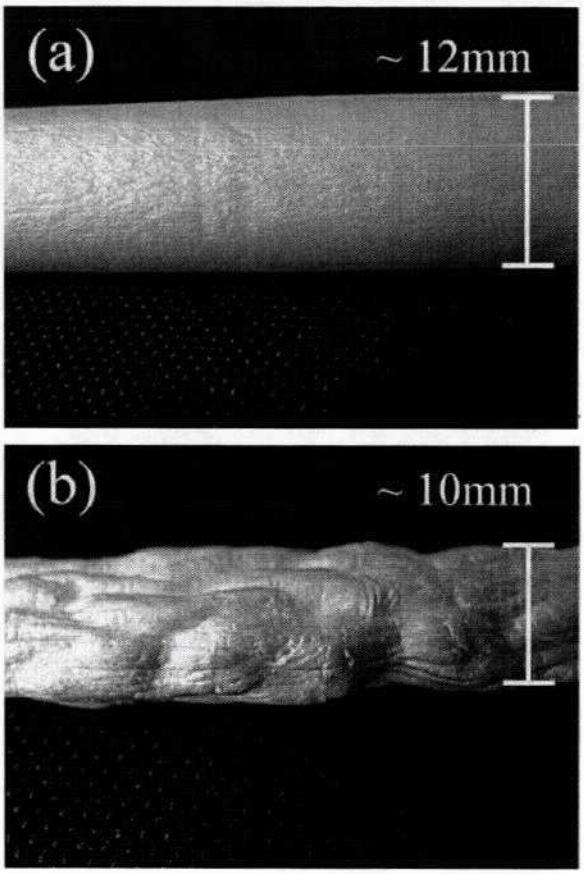

Figure 9: Macrophotographs of a PLA foam strands extruded at 100°C with 9.3 wt% CO_2; (a) as extruded, *ca.* 15 min after processing and (b) after 48h of ageing.

(a)

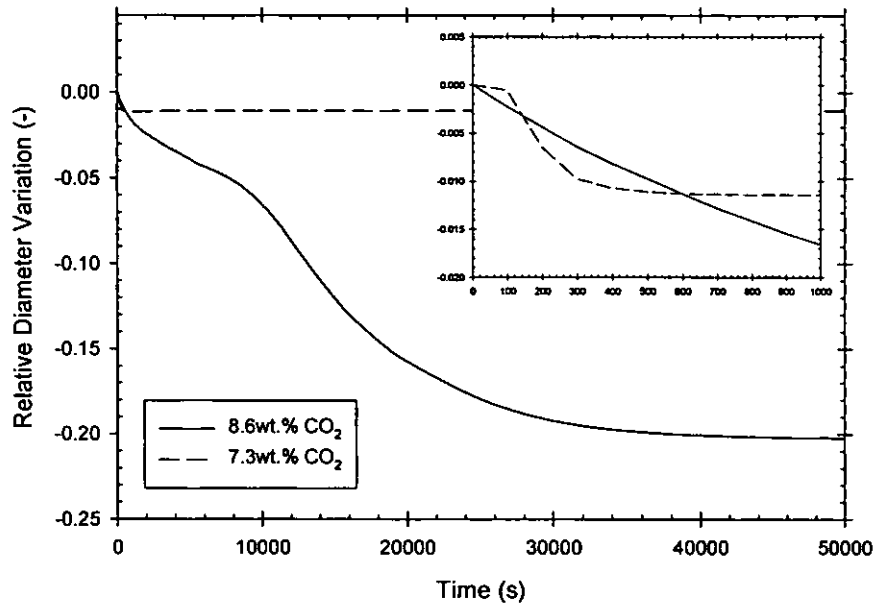

(b)

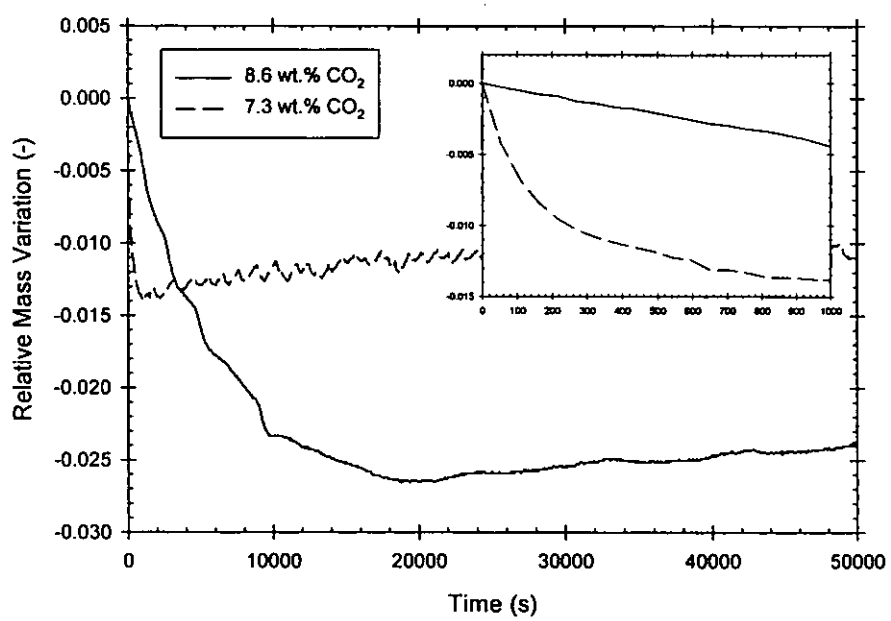

Figure 10: Relative variation of the diameter (a) and mass (b) of extruded PLA foam as a function of ageing time for blowing agent concentrations of 7.3 (dashed line) and 8.6 wt.% (solid line). The nominal temperature was set to 100°C. Inserts report detailed results obtained at shorter times.

(a)

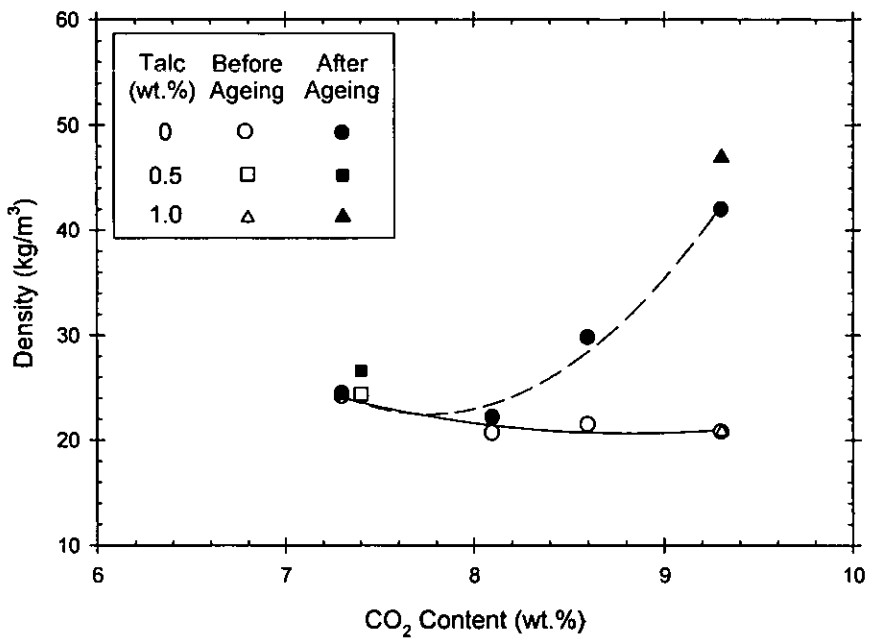
Talc (wt.%)
Before Ageing
After Ageing
0
0.5
1.0
Density (kg/m³)
CO₂ Content (wt.%)
60
50
40
30
20
10
6
7
8
9
10

(b)

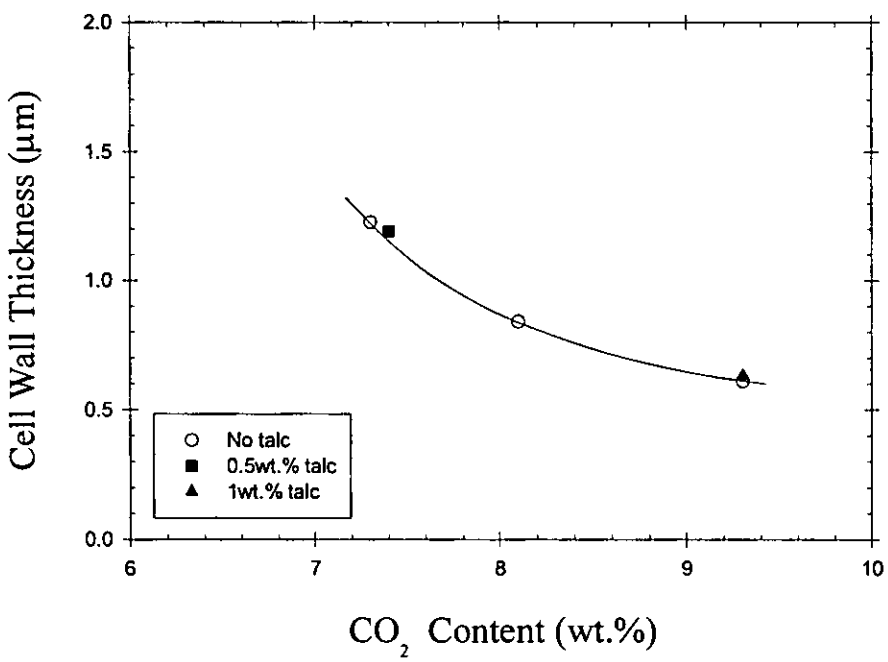
No talc
0.5wt.% talc
1wt.% talc
Cell Wall Thickness (μm)
CO₂ Content (wt.%)
2.0
1.5
1.0
0.5
0.0
6
7
8
9
10

(c)

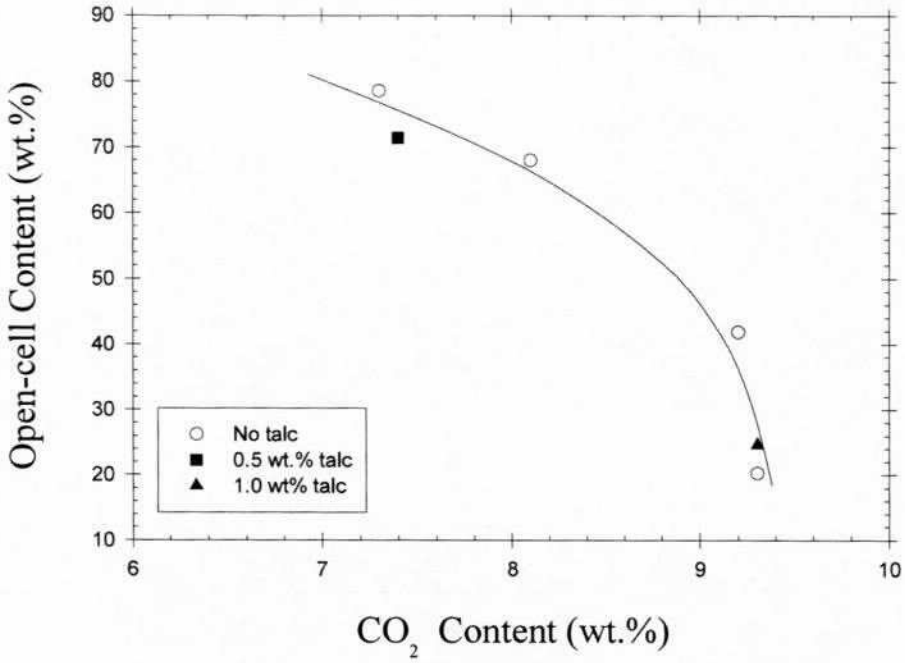

(d)

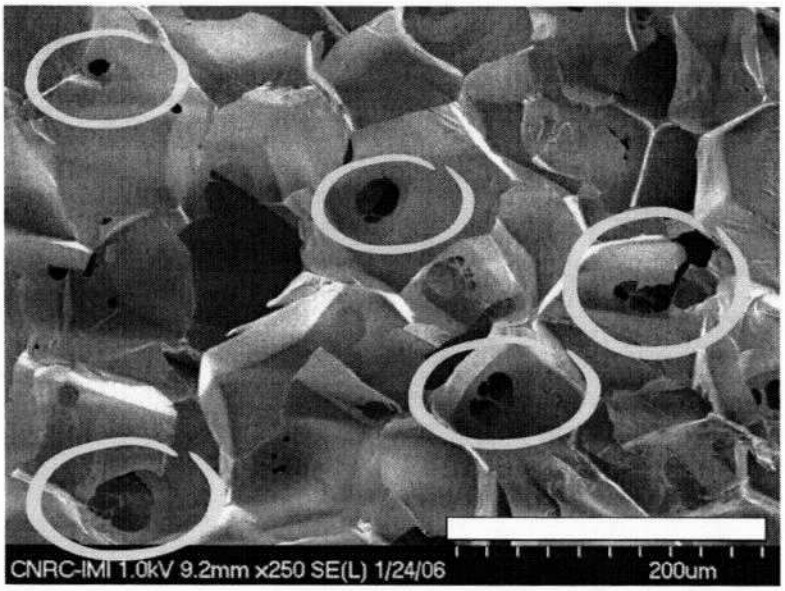

Figure 11: Effect of blowing agent concentration on (a) the bulk foam density before and after ageing; (b) the estimated cell wall thickness and (c) the open-cell content of PLA foams with CO_2 as blowing agent. The nominal temperature was set to 100°C. The lines are only guides for the eyes. (d) SEM photomicrograph of PLA foam showing several holes in cell walls. The foam was obtained at a nominal temperature of 100°C using 7.3 wt.% of CO_2. The white bar corresponds to 200 μm.

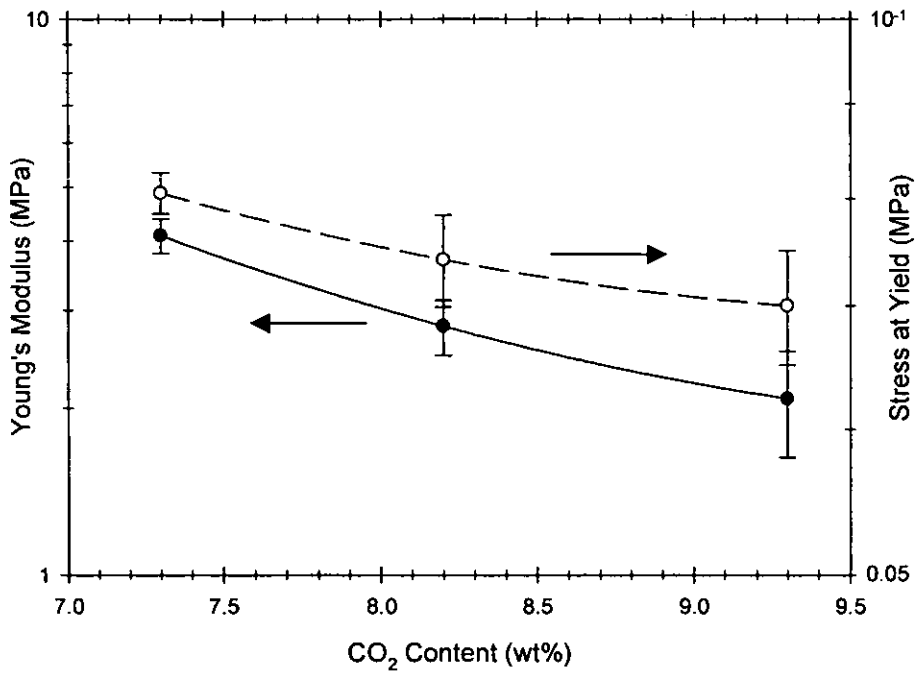

Figure 12: Compressive modulus E (filled symbols) and stress at yield σ_y (open symbols) of PLA foams as a function of the initial concentration of blowing agent used during the extrusion experiments (wt.%).